

Generalization of Rigid Foldable Quadrilateral Mesh Origami

Tomohiro TACHI*

* The University of Tokyo

7-3-1 Hongo, Bunkyo-ku, Tokyo 113-8656, Japan

ttachi@siggraph.org

Abstract

In general, a quadrilateral mesh surface does not enable a continuous rigid motion because an overconstrained system, in which the number of constraints around degree-4 vertices (three for each vertex) exceeds the number of variables (the number of hinges), is constructed. However, it is known that the developable double corrugation surface, called Miura-ori, produces a rigid deployment mechanism. The rigid-foldability of Miura-ori is due to the singularity in its pattern, where a single vertex is repeated. We generalize the geometric condition for enabling rigid motion in general quadrilateral mesh origami without the trivial repeating symmetry. To ensure the existence of a finite motion, we derive the identity of functions from the formula for degree-4 single-vertex origami. This yields a variety of unexplored generalized shapes of quadrilateral mesh origami that preserve finite rigid-foldability in addition to developability and flat-foldability.

Keywords: origami, rigid-foldability, isometric transformation, form finding

1 Introduction

Rigid-foldable origami is a piecewise linear developable surface that can realize a deployment mechanism if its facets and foldlines are substituted with rigid panels and hinges, respectively. Designing such a deployment mechanism is very important in an engineering context, particularly in architecture in the following reasons: 1) its structure based on watertight single surface is suitable for constructing an envelope of a space; 2) its purely geometric mechanism that does not rely on the elasticity of materials can contribute to a design of robust, repeatedly usable deployable structure.

The developable double corrugation surface, or Miura-ori [7], utilized in the packaging of deployable solar panels for use in space or in the folding of maps, is known to be rigid-foldable as well as developable and flat-foldable (Figure 1). Our objective is to investigate this type of quadrilateral mesh origami and generalize it so that we can obtain a design of freeform surface that is developable, flat-foldable, and rigid-foldable (Figure 6).

The developability and the flat-foldability of a piecewise linear surface are relatively easy to be generalized. The developability is represented by the gauss area (2π minus the sum of the sector angles) around each vertex to be 0. The flat-foldability is satisfied if the alternating sum of the sector angles around each vertex is 0 and the overlapping ordering can be determined, as shown by Bern and Hayes [3]. There have also been studies that analyze a valid intermediate state of origami: Huffman [5] used the gauss map to represent the valid states of an infinitesimal origami surface in three-dimensional spaces; Belcastro and Hull [2] introduced a matrix representation of the validity conditions.

On the other hand, rigid motion, i.e., the existence of a continuous path in the configuration space, has not been generalized very well. Only numerical methods have been proposed for general origami models: Watanabe and Kawaguchi [12] introduced the conditions for infinitesimal rigid-foldability by calculating the derivative (Jacobian) and the second derivative of the matrix introduced by Belcastro and Hull [2]; the author [11, 10] developed a system to calculate the folding motion of a given origami model by solving the Jacobian. However, these numerical methods cannot be used to estimate the singular finite rigid motion of Miura-ori; the reason for this is described below.

A rigid origami constructs a constrained mechanism, where the configuration is represented by the fold angle of each foldline, which is constrained by 3 equations for each inner vertex. Therefore, the infinitesimal motion can be represented by the solution space of the $3M \times N$ Jacobian matrix, where N is the number of foldlines and M is the number of the inner vertices. In this sense, a quadrilateral mesh origami constructs an overconstrained system in general because $N < 3M$. However, a Miura-ori constructs a singular $3M \times N$ matrix whose rank is $N - 1$ in every possible state, resulting in one-DOF finite rigid motion.

In this paper, we investigate this singularity and find out a method that enables it. In Section 2, we focus on a flat-foldable degree-4 origami vertex, which is known to have a special relationship between the fold angles. Then, in Section 3, we obtain the global condition that enables rigid motion and show that this is equivalent to the existence of a non-trivial valid state. Finally, a design method based on the condition is proposed in Section 4.

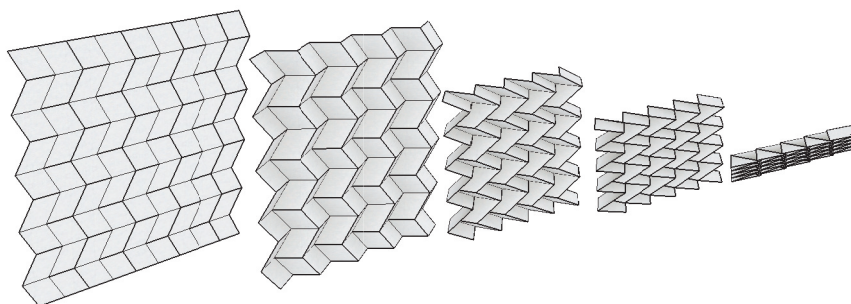


Figure 1: Rigid folding motion of Miura-ori

2 Geometry of Degree-4 Flat-foldable Vertex

The configuration of a flat-foldable degree-4 vertex can be represented by four sector angles — $\theta_A, \theta_B, \theta_C,$ and θ_D — and four folding angles — $\rho_{AB}, \rho_{BC}, \rho_{CD},$ and ρ_{DA} — between the sector angles, as shown in Figure 2. Note that ρ_{CD} is negative (mountain fold), while the other three folding angles are positive (valley fold). The crease pattern of a single vertex that satisfies the developability and the flat-foldability conditions can be represented in terms of two parameters, θ_A and θ_B ($0 < \theta_A < \pi, 0 < \theta_B < \pi, \pi \leq \theta_A + \theta_B$), as $\theta_C = \pi - \theta_A$ and $\theta_D = \pi - \theta_B$, as shown by Murata [8] and Fushimi [4]. A degree-4 single vertex rigid origami is known to have one degree of freedom. The relation between the folding angles is derived as follows using spherical trigonometry, as shown by Huffman [5] and Hull [6].

$$\rho_{CD} = -\rho_{AB} \quad \text{and} \quad \rho_{DA} = \rho_{BC} \quad (1)$$

This means that the folding angles can be represented by the two angles ρ_{AB} and ρ_{BC} , which are dependent on each other. According to Hull [6], the relationship between these two angles was derived by Robert Lang as follows:

$$\cos(\pi - \rho_{AB}) = \cos(\pi - \rho_{BC}) - \frac{\sin^2(\pi - \rho_{BC}) \sin \theta_A \sin \theta_B}{1 - \cos \xi}, \quad (2)$$

where ξ is the angle between ℓ_{AB} and ℓ_{CD} and is given by

$$\cos \xi = -\cos \theta_A \cos \theta_B + \sin \theta_A \sin \theta_B \cos(\pi - \rho_{BC}).$$

Here, we assumed that $\xi \neq 0$ to enable a one-to-one correspondence, and we will continue to make this assumption in the following sections.

Equation (2) gives a one-to-one map $f : \cos \rho_{BC} \rightarrow \cos \rho_{AB}$ as follows:

$$\cos \rho_{AB} = f(\cos \rho_{BC}) = K + \frac{1 - K^2}{\cos \rho_{BC} + K}, \quad (3)$$

where

$$K = K(\theta_A, \theta_B) = \frac{1 + \cos \theta_A \cos \theta_B}{\sin \theta_A \sin \theta_B}. \quad (4)$$

Note that map f is only dependent on a one-dimensional parameter K ($K > 1$), which is

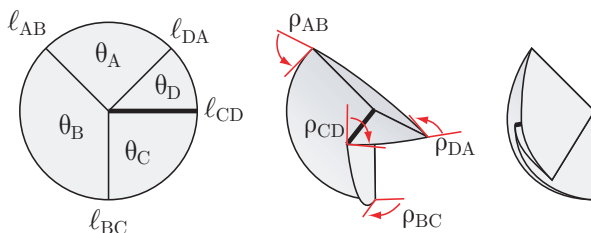


Figure 2: A flat-foldable degree-4 vertex.

determined with respect to the crease pattern. We shall call K the *conversion coefficient* of the vertex.

3 Global Condition

3.1 Valid Loop Condition

A general condition can be derived from Equation (3). The map f represents the conversion from the rotation of the lateral foldlines to the rotation of the longitudinal foldlines. Hence, its inverse $f^{-1} : \cos \rho_{AB} \rightarrow \cos \rho_{BC}$ represents the conversion from the longitudinal to the lateral foldlines. f^{-1} can be calculated from Equation (3) as follows.

$$\cos \rho_{BC} = f^{-1}(\cos \rho_{AB}) = -K + \frac{1 - K^2}{\cos \rho_{AB} - K} \quad (5)$$

According to Equations (1), the configuration of a regular quadrilateral mesh origami is represented by the cosine of the lateral and longitudinal fold angles, $\cos \rho_i^{\leftarrow}(t)$ and $\cos \rho_j^{\uparrow}(t)$ ($i = 0, 1, \dots, m - 1$ and $j = 0, 1, \dots, n - 1$), each of which is a one-dimensional function of a parameter t ($0 \leq t \leq \pi$) representing the folding motion of the entire model; m and n are the number of rows and columns of the array of inner vertices, respectively (Figure 3). The configuration is constrained at each inner vertex $v_{i,j}$ whose conversion function and coefficient are denoted by $f_{i,j}$ and $K_{i,j}$, respectively.

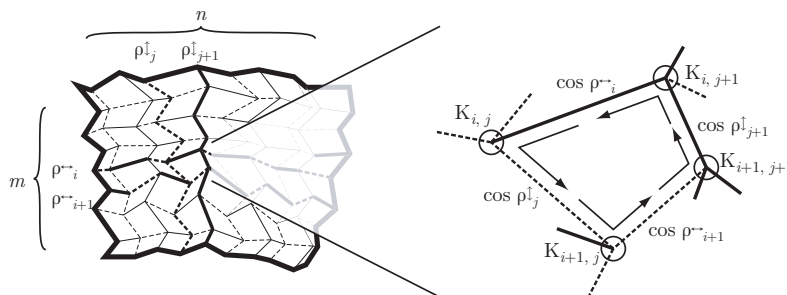


Figure 3: A quadrilateral mesh origami.

The model is rigid-foldable if and only if we can obtain $\cos \rho_i^{\leftarrow}(t)$ and $\cos \rho_j^{\uparrow}(t)$ that are consistent with Equation (3) for all inner vertices. An inconsistency can arise for the loop around an inner facet, i.e., facet whose incident vertices are not on the boundary. The fold angle of a segment determines the fold angle of the next segment, which in turn determines that of the following segment; this procedure is repeated until the fold angle of the original segment is once again determined (Figure 3 Right). Therefore, the necessary and sufficient condition for the rigid-foldability is represented as follows. For any $x = \cos \rho$ ($-\pi \leq \rho \leq \pi$), and for every inner facet surrounded by $v_{i,j}$, $v_{i+1,j}$, $v_{i+1,j+1}$, and $v_{i,j+1}$,

$$f_{i,j+1} \left(f_{i+1,j+1}^{-1} \left(f_{i+1,j} \left(f_{i,j}^{-1} (x) \right) \right) \right) \equiv \text{Identity},$$

or

$$f_{i+1,j}(f_{i,j}^{-1}(x)) \equiv f_{i+1,j+1}(f_{i,j+1}^{-1}(x)). \quad (6)$$

This can be calculated as,

$$\frac{B_j x + A_j}{A_j x + B_j} \equiv \frac{B_{j+1} x + A_{j+1}}{A_{j+1} x + B_{j+1}}, \quad (7)$$

where, for $j' = j, j + 1$,

$$\begin{aligned} A_{j'} &= -K_{i,j'} + K_{i+1,j'} \\ B_{j'} &= 1 - K_{i,j'} K_{i+1,j'}. \end{aligned}$$

This gives the following necessary and sufficient condition:

$$(A_j B_{j+1} - A_{j+1} B_j) x^2 - (A_j B_{j+1} - A_{j+1} B_j) \equiv 0, \quad (8)$$

which can be satisfied if and only if

$$A_j B_{j+1} - A_{j+1} B_j = 0 \quad (9)$$

Theorem 1 *A quadrilateral mesh origami is finitely rigid-foldable if and only if Equation (9) is satisfied for every inner facet.*

3.2 Existence of State and Existence of Motion

While the existence of a rigid motion is represented by identities, the existence of a single, static state can be represented by equalities. From the identical Equation (8), we obtain the following specific equation: For every inner quadrilateral,

$$(A_j B_{j+1} - A_{j+1} B_j) (\cos^2 \rho - 1) = 0. \quad (10)$$

This equation indicates that if there exists no rigid motion, i.e., if Equation (9) is not satisfied, a valid state can exist only if $\cos \rho = \pm 1$ (i.e., $\rho = 0, \pi, -\pi$). Here, we can conclude that the existence of rigid motion and the existence of a non-trivial state are equivalent.

Theorem 2 *A flat-foldable planar-quad mesh origami has rigid-folding motion if and only if there exists a non-trivial valid state, i.e., every foldline is folded ($\rho \neq 0$) but not completely folded ($\rho \neq \pi, -\pi$).*

4 Design

4.1 Trivial Model

It is obvious from Theorem 1 that the pattern is rigid-foldable if the conversion coefficient K of every inner vertex is constant ($K_{i,j} = K^0$). Miura-ori (Figure 1) and “MARS” (a model by Paulo Taborda Barreto [1]) (Figure 4(a)) satisfy this condition. Furthermore, if the K of every inner vertex is constant in each row or in each column ($K_{i,j} = K_i^0$ or $K_{i,j} = K_j^0$), the pattern is rigid-foldable. The single-curved Miura-ori form (Figure 4(b)) satisfies this sufficient condition.

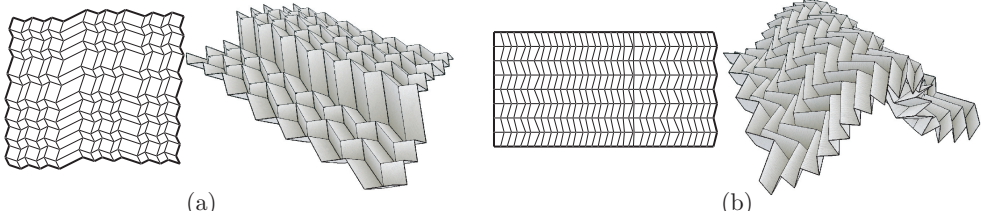


Figure 4: Rigid foldable models with trivial symmetry. (a)MARS (b)Single-curved Miura-ori.

4.2 General Model

Theorem 2 indicates that we can design a rigid-foldable origami pattern by finding a valid three-dimensional state. Here, we denote by n^{vert} , $n^{\text{inner-vert}}$, and n^{quad} , the numbers of all the vertices, the inner vertices, and the quadrilaterals, respectively. We assume that the surface is a triangular mesh so that it is represented in terms of $3n^{\text{vert}} \times 1$ vector \mathbf{x} representing the vertex coordinates. We can numerically find a valid shape by solving the following nonlinear $(2n^{\text{inner-vert}} + n^{\text{quad}}) \times 1$ vector equation with respect to \mathbf{x} :

$$\mathbf{c}(\mathbf{x}) = \begin{bmatrix} \mathbf{c}^{\text{dev}} \\ \mathbf{c}^{\text{flat}} \\ \mathbf{c}^{\text{planar}} \end{bmatrix} = \begin{bmatrix} \left[2\pi - \sum_{k=1}^4 \theta_{k,i} \right]_{n^{\text{inner-vert}} \times 1} \\ \left[\sum_{k=1}^4 (-1)^k \theta_{k,i} \right]_{n^{\text{inner-vert}} \times 1} \\ [\rho_i^{\text{crease}}]_{n^{\text{quad}} \times 1} \end{bmatrix} = \mathbf{0}, \quad (11)$$

where $\theta_{k,i}$ is the angle between k -th pair of adjacent foldlines around i -th inner vertex, and ρ_i^{crease} is the angle between the normals of two triangles consisting i -th quadrilateral. Note that $\mathbf{c}^{\text{dev}} = \mathbf{0}$ and $\mathbf{c}^{\text{flat}} = \mathbf{0}$ represent developability and flat-foldability of the surface, respectively, and $\mathbf{c}^{\text{planar}} = \mathbf{0}$ indicates that the quadrilaterals are planar.

Equation (11) yields an underdetermined system, by exploring the solution space of which we can obtain variations in the shape. We find valid shapes by starting from a trivial solution, e.g., a regular Miura-ori, and perturbing the vertex coordinates according to the null space of the Jacobian $\frac{\partial \mathbf{c}}{\partial \mathbf{x}}$, as shown in Figure 5. The Jacobian is a $(2n^{\text{inner-vert}} + n^{\text{quad}}) \times (3n^{\text{vert}})$ matrix and the solution is calculated using the pseudoinverse $[\frac{\partial \mathbf{c}}{\partial \mathbf{x}}]^+$ of the Jacobian as follows:

$$\Delta \mathbf{x} = \left(\mathbf{I} - \left[\frac{\partial \mathbf{c}}{\partial \mathbf{x}} \right]^+ \left[\frac{\partial \mathbf{c}}{\partial \mathbf{x}} \right] \right) \Delta \mathbf{x}_0, \quad (12)$$

where $\Delta \mathbf{x}_0$ represents the initial perturbation determined by an arbitrary user input. Equation (12) finds the valid perturbation closest to $\Delta \mathbf{x}_0$ by orthogonal projection to the solution space. For each step, the residual \mathbf{c} is eliminated by the Newton-Raphson method.

This method is implemented as an interactive design system in which a user can intuitively manipulate a freeform valid surface just by dragging it via a standard pointing device. Figure 6 shows the actual rigid motion of the resulting structure, animated using the rigid origami

simulator [10]. We have also observed that freeform patterns that do not satisfy our condition cannot fold without the triangulation of the quadrilateral panels.

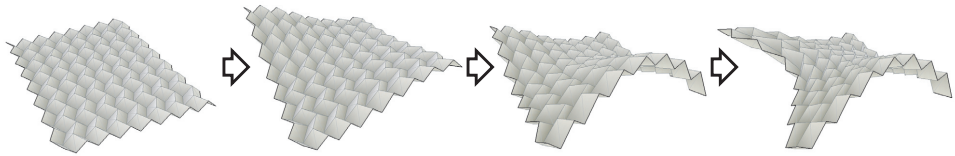


Figure 5: A perturbation within the solution space. Each form is rigid-foldable.

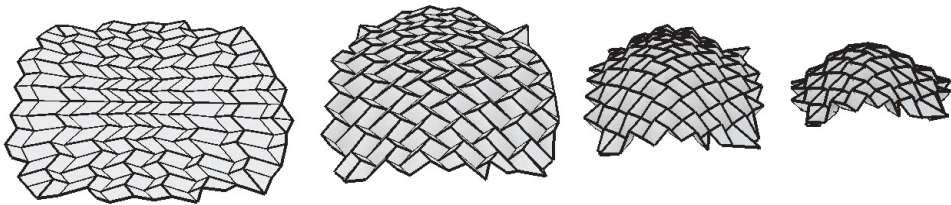


Figure 6: Freeform Miura-ori with a rigid motion.

5 Conclusion and Future Works

We have derived the necessary and sufficient condition for the existence of finite rigid motion of general flat-foldable quadrilateral mesh origami. The condition was expressed with respect to the angles in the crease pattern. We have also shown that the condition is equivalent to the existence of any non-trivial valid state. Using the condition, we have shown the method to explore freeform variations of generalized Miura-ori.

A recent study in the field of discrete differential geometry by Schief *et al.* [9] reveals the finite rigid-foldability of a quadrilateral mesh called discrete Voss surface. The singularity investigated in our study is closely related to that of discrete Voss surface. There are also other specific quadrilateral meshes known to be rigid-foldable. In the future, we intend to study on the rigid-foldability of a general quadrilateral mesh surface to unify these independently derived singular surfaces.

Acknowledgement

This research is supported by a Grant-in-Aid for JSPS Fellows funded by Japan Society for the Promotion of Science.

References

- [1] Barreto, P. T., Lines meeting on a surface: The “mars” paperfolding, In *Origami Science & Art: Proceedings of the Second International Meeting of Origami Science and Scientific Origami* (1997), pp. 343–359
- [2] Belcastro, S.-M. and Hull, T., A mathematical model for non-flat origami, In *Origami3: Proc. the 3rd International Meeting of Origami Mathematics, Science, and Education* (2002), pp. 39–51
- [3] Bern, M. and Hayes, B., The complexity of flat origami, In *Proc. the 7th Annual ACM-SIAM Symposium on Discrete Algorithms* (1996), pp. 175–183
- [4] Fushimi, K. and Fushimi, M., (1979). *Origami No Kikagaku (Geometry of Origami)*, Nihon Hyoronsha
- [5] Huffman, D., Curvature and creases: a primer on paper, *IEEE Trans.Computers*, 1976, Vol.C-25, No.10, 1010–1019
- [6] Hull, T., (2006). *Project Origami*, A K Peters
- [7] Miura, K., Proposition of pseudo-cylindrical concave polyhedral shells, In *Proceedings of IASS Symposium on Folded Plates and Prismatic Structures* (1970)
- [8] Murata, S., The theory of paper sculpture, *Bulletin of Junior College of Art*, 1966, Vol.4, 61–66, <http://ci.nii.ac.jp/naid/110004714036/>
- [9] Schief, W. K., Bobenko, A. I. and Hoffmann, T., On the integrability of infinitesimal and finite deformations of polyhedral surfaces, In *Discrete Differential Geometry (Oberwolfach Proceedings)* (2007), pp. 67–93
- [10] Tachi, T., Rigid origami simulator, 2007, <http://www.tsg.ne.jp/TT/software/>
- [11] Tachi, T., Simulation of rigid origami, In *Origami⁴: Proceedings of The Fourth International Conference on Origami in Science, Mathematics, and Education* (2009), to appear
- [12] Watanabe, N. and Kawaguchi, K., The method for judging rigid foldability, In *Origami⁴: Proceedings of The Fourth International Conference on Origami in Science, Mathematics, and Education* (2009), to appear